Superparamagnetic Triblock Copolymer/Fe_2O_3 Hybrid Nanofibers**

Xiaohu Yan, Guojun Liu,* Futian Liu,
Ben Zhong Tang, Han Peng, Alexander B. Pakhomov,
and Catherine Y. Wong

Block copolymers self-assemble in bulk to form various intricate nanometer-sized block segregation patterns.[1] Block-segregated structures of diblock copolymers have been processed chemically to yield nanofibers,[2,3] nanospheres,[4] and nanochannels in thin films.[5, 6] Here we report on the preparation of polymer/Fe_2O_3 hybrid nanofibers by processing films of the triblock copolymer polystyrene-*block*-poly(2-cinnamoyloxyethyl methacrylate)-*block*-poly(*tert*-butyl acrylate) or PS-*b*-PCEMA-*b*-P*t*BA.

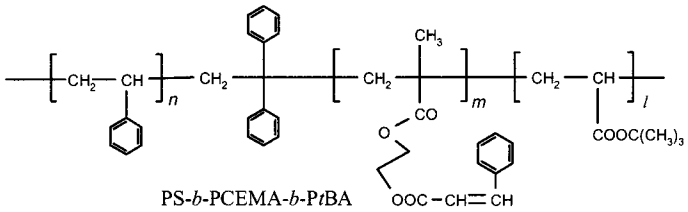

The preparation involved the self-assembly of the blocks in thin films into concentric PCEMA and P*t*BA cylinders dispersed in a matrix of PS (A →B in Scheme 1). The cylindrical structures were then locked in by photo-cross-linking the PCEMA shells (B →C). Dissolving the films in THF yielded individual nanofibers with PS coronas, PCEMA middle layers, and P*t*BA cores (C →D). Nanotubes with PAA-lined cores [PAA = poly(acrylic acid)] were obtained by cleaving the *tert*-butyl groups from P*t*BA (D →E). Producing Fe_2O_3 nanoparticles in the PAA cores yielded solvent-dispersible superparamagnetic block copolymer/inorganic hybrid nanofibers (E →F).

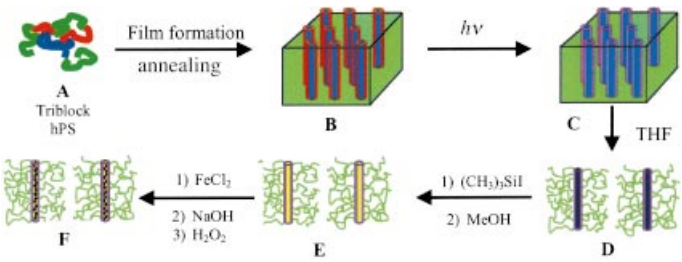

Scheme 1. Preparation of the triblock copolymer/Fe_2O_3 hybrid nanofibers (see text for details).

The triblock copolymer used consisted of 690 styrene, 170 CEMA, and 200 *t*BA units. Films were obtained by evaporating a toluene solution containing the triblock copolymer and a homopolystyrene (hPS) standard. Figure 1 shows a transmission electron microscopy (TEM) image of a 50-nm-thick section of such a film stained with OsO_4. On the right of the image, concentric ellipses with short stems dominate. These represent projections of cylinders, deformed along the microtoming direction, with PCEMA shells and P*t*BA cores aligned slightly off the normal direction of the image. The PCEMA shells appear darker, because OsO_4 reacted with PCEMA selectively. The diameter of such P*t*BA cores is about 20 nm, which is smaller than the average contour length of about 50 nm for the P*t*BA chains. On the left of Figure 1 some cylinders lie in the plane of the picture.

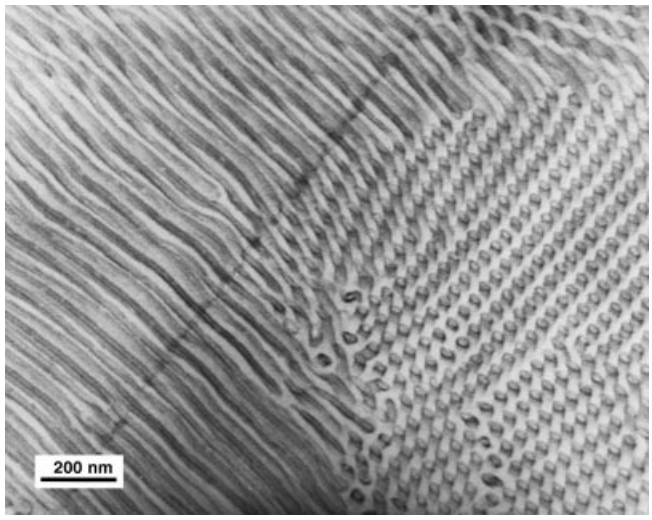

Figure 1. TEM image of a 50-nm-thick section of a PS-*b*-PCEMA-*b*-P*t*BA/hPS film. The sample was stained with OsO_4 vapor. TEM was performed at 70 kV with a Hitachi H-7000 instrument.

The PCEMA was cross-linked by dimerization between CEMA units of different chains with light from a mercury lamp that had passed through a 290-nm cut-off filter.[7] A typical CEMA conversion of 22%, measured by FTIR spectroscopy, was used in this study. Such irradiated triblock/hPS films disintegrated in THF under gentle stirring due to the separation of cross-linked cylindrical domains and

[*] Prof. G. Liu,[+] Dr. X. Yan, F. Liu
Department of Chemistry, University of Calgary
2500 University Dr., NW, Calgary, AB, T2N 1N4 (Canada)
Fax: (+1) 403-289-9488
E-mail: gliu@ucalgary.ca

[+] The State Key Laboratory of Functional Materials for Adsorption and Separation
Nankai University, Tianjin (China)

Dr. B. Z. Tang, H. Peng
Department of Chemistry, Hong Kong University of Science & Technology
Clear Water Bay, Kowloon (Hong Kong)

Dr. A. B. Pakhomov, C. Y. Wong
Magnetics Innovation Center, Materials Characterization and Preparation Facility
Hong Kong University of Science & Technology (Hong Kong)

[**] NSERC of Canada is acknowledged for sponsoring this research. Dr. R. Yamdagni and Ms. Q. Wu are thanked for help with the use of their NMR magnet. Dr. Zhao Li is thanked for performing the TGA analysis. G.L. thanks the NSF of China for a distinguished Young Investigator's grant.

  1433-7851/01/4019-3593 $ 17.50+.50/0

formation of isolated nanofibers in THF. The cleavage of the *tert*-butyl groups was accomplished by a method used extensively by us in the past.[2] It involved treating the PS-*b*-PCEMA-*b*-P*t*BA nanofibers with $(CH_3)_3SiI$ and then decomposing the excess $(CH_3)_3SiI$ with methanol containing about 2% water. Quantitative removal of the *tert*-butyl groups was confirmed by FTIR studies, and the morphologies of the PS-*b*-PCEMA-*b*-P*t*BA nanofibers and PS-*b*-PCEMA-*b*-PAA nanotubes were confirmed by TEM studies.

A literature method[8] was followed to load the PAA-lined PS-*b*-PCEMA-*b*-PAA nanotubes with presumably γ-Fe_2O_3. After Fe_2O_3 loading, the nanofiber dispersion became red. Nanofibers prepared after Fe_2O_3 loading had a Fe_2O_3 content of about 0.28 g per gram of nanofibers, as determined by thermogravimetric analysis. These fibers remained dispersed for days in THF or other organic solvents that solubilize PS. Figure 2a shows a TEM image of such fibers sprayed onto carbon-coated copper grids. Since the fibers were not stained before TEM observation, Fe_2O_3 must constitute the visible part of the fibers. The diameter of the Fe_2O_3-impregnated portion is about 20 nm, which is the same as that of the P*t*BA cores shown in Figure 1 and suggests synthesis of Fe_2O_3 inside the PAA cores. Figure 2b shows an image of the hybrid fibers taken at a higher magnification. The encapsulating layers are clearly visible here.

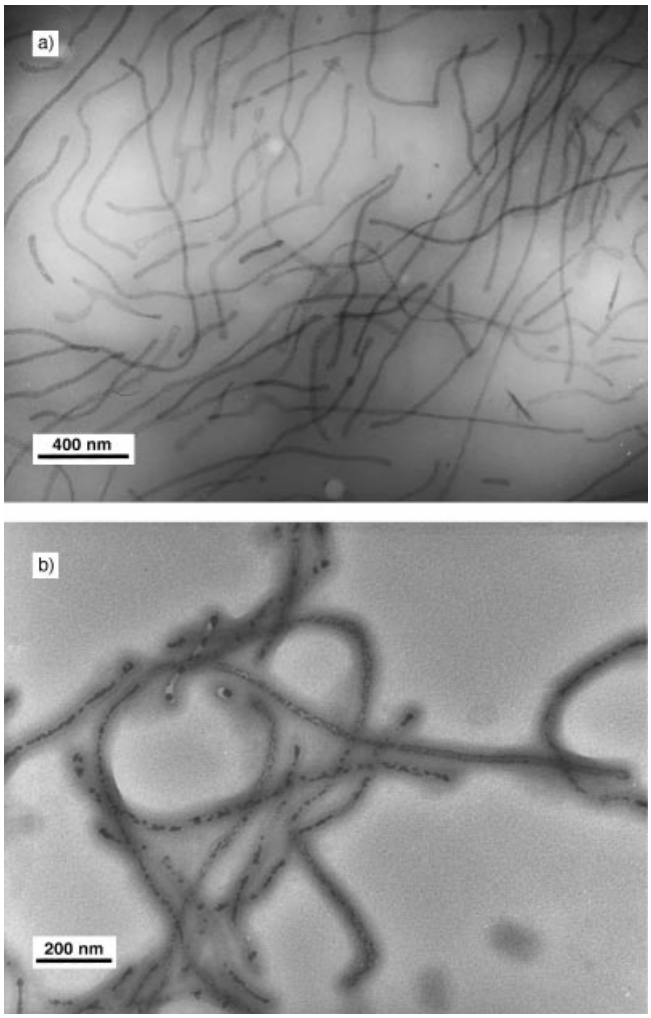

Figure 2. TEM images of triblock/Fe_2O_3 hybrid nanofibers at different magnifications. A THF solution of the sample was aspirated onto a carbon-coated copper grid to prepare the specimen. The samples were not stained.

We obtained electron-diffraction data for the Fe_2O_3 particles. Due to the similarity of the interplanar distances in the different crystalline forms of Fe_2O_3, we could not conclude unambiguously that the particles were γ-Fe_2O_3. Figure 3a shows magnetization curves for the hybrid nanofibers, measured with a SQUID magnetometer (Quantum Design MPMS-5S) at 10, 100, 200, and 300 K. Only at 10 K was measurable coercivity obtained, that is, the particles are superparamagnetic. However, the saturation magnetization at 300 K was low (0.24 emu per gram of hybrid nanofibers or 0.86 emu per gram of iron oxide), but it increased with decreasing temperature and reached about 11.4 emu per gram of Fe_2O_3 at 10 K. Figure 3b depicts the variation in the magnetization of a hybrid fiber sample at 500 G as a function of temperature under zero-field-cooled (ZFC) and field-cooled (FC) conditions. While the field of 500 G was applied after the sample had been cooled to 10 K in the ZFC case, the field was applied

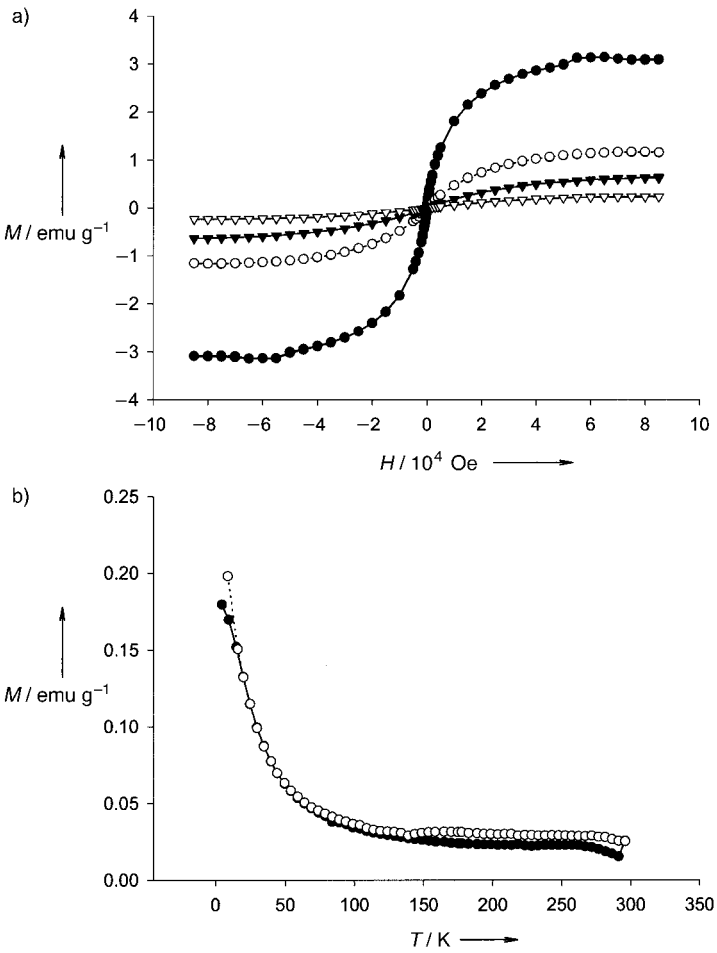

Figure 3. a) Magnetization curves of the hybrid nanofibers at 300 K (▽), 200 K (▼), 100 K (○), and 10 K (●). b) Magnetization at 500 G as a function of temperature under ZFC (●) and FC (○) conditions.

  1433-7851/01/4019-3594 $ 17.50+.50/0

at room temperature before sample cooling to 10 K and then warming to 300 K again in the FC case. For γ-Fe_2O_3 particles prepared previously in polymer matrices,[9] the ZFC magnetizations at low temperature were much lower than the FC magnetizations, because the particles became magnetically frozen, and their magnetic moment could not flip and align rapidly along the direction of the applied field under ZFC conditions. Only above a blocking temperature[10] could the spins flip, and the ZFC magnetization then coincided with the FC magnetization. Such a blocking temperature is definitely not observed in our case in the range 10 – 300 K. The drastic increase in saturation magnetization with decreasing temperature and a blocking temperature below 10 K suggest that our Fe_2O_3 particles are small (that is, < 5 nm). Small particles were probably formed due to the use of THF/water rather than water as the solvent during Fe_2O_3 preparation. Alternatively, the abnormal behavior may be due to contamination of the magnetic γ-Fe_2O_3 by other forms of Fe_2O_3.

Due to the low magnetization of the hybrid fibers at room temperature, the as-made fibers may not be useful as magnetic materials. The more gratifying aspect is the ability of the inorganic particles to modify the properties of the polymer fibers. For example, we dispersed the hybrid fibers in a mixture consisting of 28.9 wt % of THF, 58.7 wt % of styrene, 10.4 wt % of divinylbenzene, and 2.0 wt % of benzoyl peroxide in an NMR tube. After the mixture had equilibrated in the uniform 4.7-T field of a Varian XL-200 NMR spectrometer for 3 h at room temperature, the temperature was raised to 70 °C to gel the matrix. Figure 4 shows a

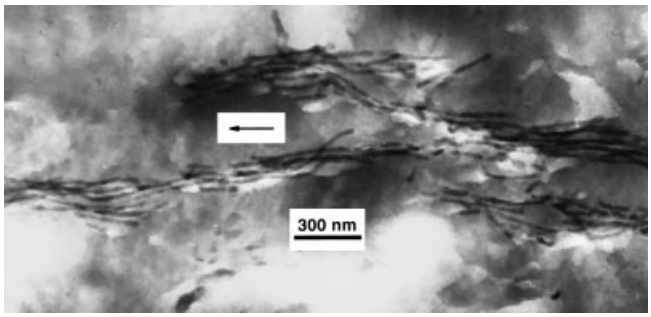

Figure 4. Side view of the hybrid fibers aligned in the magnetic field. The rugged background is due to partial shattering of cross-linked PS during microtoming.

representative TEM image of a thin section microtomed from the cylindrically shaped sample thus gelled in the NMR tube. The hybrid fibers are aligned along the direction of the magnetic field (arrow). Since no alignment or bundling was observed for the PS-*b*-PCEMA-*b*-PAA nanotubes under similar conditions, alignment of the hybrid nanofibers was probably due to the magnetic anisotropy of the Fe_2O_3 particles produced in the PAA-lined cores of the triblock tubes. Further experiments will involve obtaining the magnetization curves of such aligned fibers parallel and perpendicular to their axial direction to determine this anisotropy.[11]

We also examined the phase-segregation properties of solutions of the hybrid nanofibers and the PS-*b*-PCEMA-*b*-PAA nanotubes in THF after solvent evaporation with and without an applied magnetic field. Figure 5 shows a TEM image of a thin section obtained after microtoming such a film that was dried immediately next to the NMR solenoid. The magnetic fibers are not fully aligned here because of the weaker field, but phase separation occurred. No phase

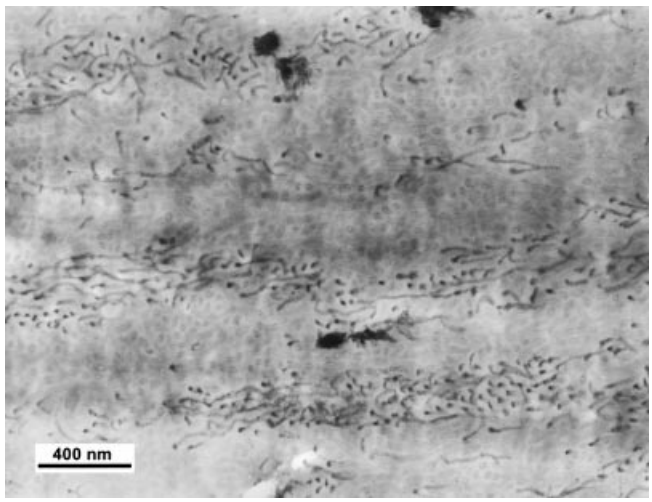

Figure 5. TEM images of a 50-nm-thick section of a PS-*b*-PCEMA-*b*-PAA nanotube and hybrid fiber film dried in a magnetic field. The sample was not stained.

separation was observed when such a sample was dried in the absence of an applied magnetic field. Thich is in agreement with the fact that the enthalpy of mixing of the hybrid fibers and tubes should be close to zero under such circumstances. The more intriguing aspect is that the fibers and tubes formed alternating multilayers (Figure 5). We do not yet know whether we can make periodically spaced layers. Films containing such layers may serve as photonic crystals.[12]

In summary, we have produced solvent-dispersible PAA-lined PS-*b*-PCEMA-*b*-PAA nanotubes and polymer/Fe_2O_3 hybrid nanofibers. Such hybrid fibers aligned and segregated from the PS-*b*-PCEMA-*b*-PAA nanotubes in a magnetic field. Superparamagetic particles were prepared previously in polymer films,[9, 13], polymer gel particles,[14] in microemulsion droplets,[15] and in lipid vesicles.[16] Preparation of magnetic nanofibers in the channels of ion-track-etched membranes[11] or anodized alumina[17] and in tubes of conductive polymers has also been reported.[18] To our knowledge, this the first report on the preparation of superparamagnetic Fe_2O_3 nanoparticles in solvent-dispersible block copolymer nanotubes.

Experimental Section

The triblock copolymer was prepared by anionic polymerization by following procedures used by us previously to synthesize PS-*b*-PCEMA[2] and PCEMA-*b*-P*t*BA[5] diblock copolymers. Light scattering in chloroform using the measured specific refractive index increment of $0.122\ mL\,g^{-1}$ yielded a weight-average molecular mass of $1.42 \times 10^5\ g\,mol^{-1}$ for the sample. Comparing intensities of the ^1H peaks of the three blocks gave $n:m:l = 1.00:0.25:0.29$. Gel-permeation chromatography in THF with a poly(methyl methacrylate) standards gave a polydispersity of 1.13 for the

  1433-7851/01/4019-3595 $ 17.50+.50/0

triblock copolymer. Triblock copolymer films were obtained by evaporating a concentrated toluene solution of the copolymer and a hPS standard ($\bar{M}_w = 2500\ g\,mol^{-1}$, $\bar{M}_w/\bar{M}_n = 1.09$) in a mass ratio of 1.00/0.40 over 3 d. The films were then annealed at 120 °C for one week. To incorporate Fe_2O_3, an excess of $FeCl_2$ was equilibrated with the nanotubes with PAA-lined cores in deoxygenated THF. The excess $FeCl_2$ was removed after precipitation of the Fe^{2+}-impregnated tubes into methanol. The trapped Fe^{2+} was then treated with NaOH in THF containing 2 % water to form iron(II) hydroxide or oxide. Fe_2O_3 was prepared by oxidizing the iron(II) hydroxide or oxide with hydrogen peroxide.

Received: May 14, 2001 [Z17109]

[1] F. S. Bates, G. H. Fredrickson, *Phys. Today* **1999**, *51*(2), 32.
[2] G. J. Liu, J. Ding, L. Qiao, A. Guo, J. T. Gleeson, B. Dymov, T. Hashimoto, K. Saijo, *Chem. Eur. J.* **1999**, *5*, 2740.
[3] J. Massey, K. N. Power, I. Manners, M. A. Winnik, *J. Am. Chem. Soc.* **1998**, *120*, 9533.
[4] K. Ishizu, A. Onen, *J. Polym. Sci. A* **1989**, *27*, 3719.
[5] G. J. Liu, J. Ding, T. Hashimoto, K. Saijo, F. M. Winnik, S. Nigam, *Chem. Mater.* **1999**, *11*, 2233.
[6] J.-S. Lee, A. Hirao, S. Nakahama, *Macromolecules* **1989**, *22*, 2602.
[7] M. Kato, T. Ichijo, K. Ishii, M. Hasegawa, *J. Polym. Sci. A* **1971**, *9*, 2109.
[8] R. F. Ziolo, E. P. Giannelis, B. A. Weinstein, M. P. O'Horo, B. N. Ganguly, V. Mehrotra, M. W. Russell, D. R. Huffman, *Science* **1992**, *257*, 219.
[9] a) B. H. Sohn, R. E. Cohen, *Chem. Mater.* **1997**, *9*, 264; b) B. Z. Tang, Y. H. Geng, J. W. Y. Lam, B. S. Li, X. B. Jing, X. H. Wang, F. S. Wang, A. B. Pakhomov, X. X. Zhang, *Chem. Mater.* **1999**, *11*, 1581.
[10] L. Neel, *Rev. Mod. Phys.* **1953**, *25*, 293.
[11] T. M. Whitney, J. S. Jiang, P. C. Searson, C. L. Chien, *Science* **1993**, *261*, 1316.
[12] A. Urbas, R. Sharp, Y. Fink, E. L. Thomas, M. Xenidou, L. J. Fetters, *Adv. Mater.* **2000**, *12*, 812.
[13] a) K. Yamaguchi, T. Sato, Y. Kato, M. Inoue, T. Fujii, *Mater. Sci. Forum* **1998**, *287–288*, 483; b) O. Jarjayes, P. H. Fries, G. Bidan, *J. Magn. Magn. Mater.* **1994**, *137*, 205.
[14] E. Kroll, F. M. Winnik, R. F. Ziolo, *Chem. Mater.* **1996**, *8*, 1594.
[15] J. A. Lopez-Perez, M. A. Lopez-Quintela, J. Mira, J. Rivas, S. W. Charles, *Phys. Chem. B* **1997**, *101*, 8045.
[16] a) S. Mann, J. Skarnulis, R. J. P. William, *J. Chem. Soc. Chem. Commun.* **1979**, 1030; b) I. I. Yaaco, A. C. Nunes, A. Bose, *J. Colloid Interface Sci.* **1995**, *171*, 73.
[17] R. M. Metzger, V. V. Konovalov, M. Sun, T. Xu, G. Zangari, B. Xu, M. Benakli, W. D. Doyle, *IEEE Trans. Magn.* **2000**, *36*, 30.
[18] H. Cao, Z. Xu, H. Sang, D. Sheng, C. Tie, *Adv. Mater.* **2001**, *13*, 121.

Thermally Stable Homogeneous Catalysts for Alkane Dehydrogenation**

Matthias W. Haenel,* Stephan Oevers, Klaus Angermund, William C. Kaska,* Hua-Jun Fan, and Michael B. Hall*

Dedicated to Professor Heinz A. Staab on the occasion of his 75th birthday

Thermostable homogeneous catalysts have three major advantages: the first is that less reactive substrates, for which the kinetics require high temperatures, can be transformed to products; second, they expand the field of homogeneous catalysis to include more endothermic processes, for which the thermodynamics require high temperatures; the third benefit is facile catalyst separation by distillation of educts and products. A process where such catalysts would definitely show great promise is the C–H activation of alkanes in homogeneous solution with dehydrogenation to alkenes and hydrogen.[1] However, thermostable homogeneous catalysts for endothermic processes are almost nonexistent[2] and the synthesis of suitable organometallic coordination compounds seemed destined to be abandoned because of complex instability at high temperatures.[3] This trend was reversed with the introduction of tridentate coordination compounds[4] in the form of PCP pincer complexes $[MCl(H)\{C_6H_3(CH_2PtBu_2)_2\text{-}2,6\}]$ (**1**, **2**)[5] and their subsequent conversion into $[M(H)_2\{C_6H_3(CH_2PtBu_2)_2\text{-}2,6\}]$ and $[M(H)_4\{C_6H_3(CH_2PtBu_2)_2\text{-}2,6\}]$ (M = Rh, Ir).[6, 7] The transition metal dihydrides, especially the iridium compounds **3** and **4**, are thermally stable up to 200 °C and are reactive to aliphatic and cycloaliphatic C–H bonds.[7]

An even higher thermostability can be expected for "anthraphos" complexes **6** and **7** which are obtained by replacing the benzylic PCP pincer ligands with anthracene-

[*] Prof. Dr. M. W. Haenel, Dr. S. Oevers, Dr. K. Angermund
Max-Planck-Institut für Kohlenforschung
Kaiser-Wilhelm-Platz 1
45470 Mülheim an der Ruhr (Germany)
Fax: (+49) 208-3062980
E-mail: haenel@mpi-muelheim.mpg.de

Prof. Dr. W. C. Kaska
Department of Chemistry
University of California Santa Barbara
Santa Barbara, CA 93106 (USA)
Fax: (+1) 805-8934120
E-mail: kaska@chem.ucsb.edu

Prof. Dr. M. B. Hall, Dr. H.-J. Fan
Department of Chemistry
Texas A&M University
3255 TAMU, College Station, TX 77843-3255 (USA)
Fax: (+1) 979-8452971
E-mail: hall@mail.chem.tamu.edu

[**] S.O. thanks the German Academic Exchange Service (DAAD) for financing a research stay with W.C.K. in the USA. This work was supported by the National Science Foundation (CHE 9800184 to M.B.H.), by the University of California Energy Institute and University of California Santa Barbara (to W.C.K.), and by the German Research Association (DFG, to M.W.H). We thank Dr. R. Mynott and Mrs. C. Wirtz, MPI für Kohlenforschung, for NMR spectroscopic investigations.

  1433-7851/01/4019-3596 $ 17.50+.50/0